

BIOSORPTION OF Cu (II) IONS USING RESIDUAL TOMATO POMACE BIOMASS. A STUDY OF ISOTHERMS AND KINETICS

Cerasella INDOLEAN^{a*}, Silvia BURCĂ^a

ABSTRACT. This work investigates the possible usage of tomato pomace biomass (TPB) as support for metabolic quantities of copper. Thus, biosorption potential of natural and biodegradable matrix formed from tomato residue, in suspension form was explored. The effect of biomass quantity, Cu(II) concentration and temperature were assessed.

Analysis of Fourier-transform infrared (FTIR) spectrum, scanning electron microscopy (SEM) images and elemental analysis suggested that the organic functional groups take part in the Cu (II) biosorption process, and some surface modifications and appearance of cavities onto the TPB surface were observed after biosorption.

Experimental data were analysed in terms of pseudo-first order, pseudo-second order, intraparticle diffusion and external diffusion kinetic models. The results showed that the biosorption process of Cu(II) ions followed well pseudo-second order kinetics. The biosorption data of Cu(II) ions at 295 K are fitted to Langmuir, Freundlich, Dubinin–Radushkevich (D–R) and Temkin isotherms. Biosorption of Cu(II) onto TPB followed the Freundlich isotherm model ($R^2 = 0.93$) with the maximum biosorption capacity of 2.05 mg/g. In conclusion, TPB showed appropriate adsorption capacity, 0.5 g of this biomaterial, as powder, containing Cu(II), could be used as a dietary supplement in order to supply the daily copper demand of the organism.

Keywords: *Lycopersicon esculentum*, tomato pomace biomass, Cu(II), lycopene, biosorption, dietary supplement

^a Babeş-Bolyai University, Faculty of Chemistry and Chemical Engineering, 11 Arany Janos str., RO-400028, Cluj-Napoca, Romania

* Corresponding author: liliana.indolean@ubbcluj.ro



INTRODUCTION

As one of the most popular vegetables in the world, tomatoes (*Lycopersicon esculentum*) are rich in lycopene, phenolics, organic acids, vitamins and many other beneficial components [1,2]. As is known, the tomatoes can be served as fresh vegetables or, as some processed products, such as paste, juice, sauce, puree and ketchup. In industry, processed tomatoes generate about 10–40% of by-products containing peel, seeds, as well as a small amount of pulp, known as tomato pomace, which is widely known as a rich source of β -carotene and lycopene [3]. Utilization of tomato pomace has been limited. Most studies have involved organic extraction of antioxidants from tomato peels, as over 50% antioxidants in tomato are in peels and seeds, and tomato peels have three times more lycopene, one of the major tomato antioxidants than whole tomato [4].

Every year, the alimentary industry generates significant amounts of tomato residues, in many cases considered as wastes, responsible of disposal problems and environmental pollution. In fact, the accumulation of these residues, predominantly in the warm periods, promotes uncontrolled anaerobic fermentations leading to environmental problems [5].

Copper, Cu (II), is an essential trace element in both humans and animals, required as a cofactor and/or structural component of numerous metalloenzymes. It uses copper to form red blood cells, bone and connective tissue. Copper is also involved in the processing of cholesterol, the proper functioning of your immune system and the growth and development of babies in the womb. [6]

The body of a healthy adult contains approximately 80–100 mg of copper, accumulated mainly in the bones, liver, and muscles [7].

The World Health Organization (WHO) and the Food and Agriculture Administration (FAA) suggest that the average daily intake of copper for a healthy adult should not exceed 0.9 mg/day, while during pregnancy it should be 1.0 mg/day and 1.3 mg/day during breastfeeding for women [6]. The food sources of copper include meat, crustaceans, nuts, wholemeal foods, and dried fruit. Around 50% of copper is absorbed in the stomach, duodenum, and the initial parts of the small intestine, and the remaining amount is excreted in faeces [7,8].

For this reason, the aim of this research is to purpose obtaining a functional food based on Cu(II), in metabolic quantity, biosorbed onto a tomato biomass waste matrix, rich in antioxidants, cheap and available from local alimentary industry.

The variables operation effect such as initial copper ion concentration, adsorbent dose, contact time and stirring rate were investigated.

RESULTS AND DISCUSSION

I. Biosorbent characterization

1.1. Fourier transform infrared spectroscopy (FTIR)

FTIR spectra were recorded using JASCO 615 FTIR spectrometer. The sample of dried biosorbents was grinded sufficiently with KBr by pallet method. The spectra were recorded in the range of 500–4000 cm^{-1} and resolution 2 cm^{-1} .

In Figure 1 are depicted the spectra of TPB before and after Cu(II) adsorption. The broad absorption peak at around 3255.2 cm^{-1} corresponds to the O–H stretching vibrations due to inter- and intra-molecular hydrogen bonding of polymeric compounds (macromolecular associations), such as alcohols, phenols and carboxylic acids, as in pectin, cellulose and lignin, thus, showing the presence of hydroxyl groups on the adsorbent surface [8]. After Cu(II) biosorption this band was shifted at 3261 cm^{-1} , fact which supports the Cu(II) presence onto TPB surface. The sharp bands at 2915.8 cm^{-1} and 2850 cm^{-1} can be attributed to the aliphatic saturated C-H stretching vibrations of the lignin, cellulose and hemicellulose polysaccharides. The presence of the peak at 1619.9 cm^{-1} indicates the carbonyl (C=O) stretching vibration of the carboxyl groups of pectin, hemicellulose and lignin, peak that was shifted at 1706.6 cm^{-1} after Cu (II) biosorption, fact that confirm the presence of the metal in the biomass structure [8,9]. The other prominent band is due to C=O (carbonyl) group, at 1022.08 cm^{-1} that was shifted at 1024.01 cm^{-1} . Moreover, in the case of TPB, after Cu(II) biosorption, a remarkable modification in positions and amplitude of –OH and C=O bands was observed, which indicates that Cu(II) was linked mostly at these groups, and it can be seen that some of the characteristic absorption bands of TPB biomass after biosorption were shifted at higher values than those of TPB before biosorption [10-12].

Peaks in the wavenumber region below 800 cm^{-1} can be attributed to the presence of bioligands. These spectra indicate that the studied biosorbent contains a wide variety of functional groups such as hydroxyl, carboxyl, amides, ethers, ketones, and esters that play important role for Cu (II) binding through different mechanisms. The changes in FTIR spectra confirm the binding of Cu with functional groups present in the biosorbent. Similar observations were also reported by Pandya et al. [13].

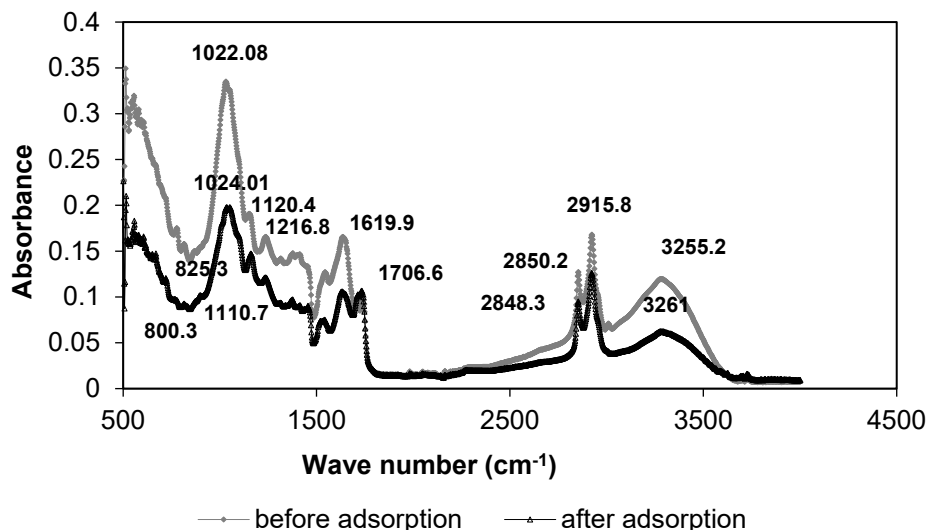


Figure 1. FTIR spectra before Cu (II) biosorption onto TPB (grey line) and after biosorption (black line).

1.2. Elemental analysis

Elemental analysis (EA) is, as is well-known, an analytical technique applied in chemistry to determine the elemental composition of chemical compounds and their composites.

The composition of the TPB sample was characterised by means of proximate and ultimate analyses. Elemental (C, H and N) analysis was performed using a Perkin Elmer PE2400 CHNS/O Elemental Analyzer.

The oxygen content was calculated by difference from the data obtained by the Perkin Elmer PE 2400 CHNS/O Elemental Analyzer machine.

Elemental composition (wt.% on dry basis) for TPB was % C = 45.77; % H = 6.67; % N = 3.35; % S = 0.14.

The results of elemental analysis reveal that TPB has high carbon content, which makes it a good precursor material for biosorbents.

1.3. Scanning Electron Microscope (SEM) analysis

Scanning electron microscopy (SEM) images for samples were obtained with a JEOL (USA) JSM 5510 LV apparatus. Prior to analyse, biosorbent samples were mounted on a stainless stab with a double stick tape. Then they were coated with a thin layer of gold under vacuum to improve electron conductivity and image quality.

In order to examine the morphological structure of biomass, SEM micrographs of TPB were taken before and after Cu (II) biosorption and presented in Figure 2. SEM micrograph of initial TPB material indicates a smooth structure of the biomass surface, Figure 2a. After metal loading, some surface modification and appearance of cavities onto the TPB surface were observed, Figure 2b.

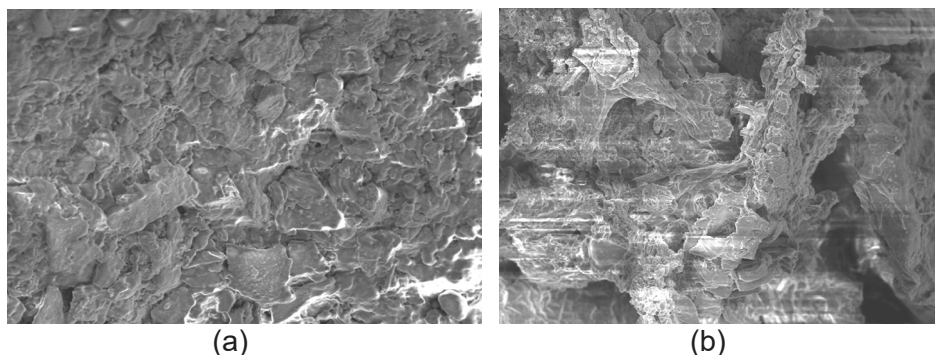


Figure 2. SEM micrograph (x1000) of (a) TPB before and (b) after Cu(II) biosorption.

II. Biosorption study

II.1. Effect of Cu(II) concentration on the biosorption process

Cu(II) concentration influence was studied using the following biosorption conditions: 1g TPB, $d = 200-400 \mu\text{m}$, 296 K, $\text{pH} = 5.41$, 300 rpm, contact time 240 min, with concentrations in 12.5-68 mg Cu(II)/L range. Time evolution was also followed for all concentrations used.

Experimental results showed that sorption capacity increases with increasing concentration of Cu^{2+} ions in aqueous solution, from 0.285 mg/g when a 12.5 mg Cu^{2+} /L aqueous solution was used up to 1.98 mg/g when a 68 mg Cu^{2+} /L aqueous solution was used, Figure 4. But as the initial concentration increases, sorption process equilibrium was reached more difficult, after about 125 minutes, by comparison with just 30 minutes for small concentrations (12.5 – 27.5 mg Cu^{2+} /L), Figure 3. However, for further experiments was chosen the initial metal concentration to be 68 mg Cu(II)/L, because the biosorption efficiency was the highest.

In addition, this value of 1.98 mg Cu^{2+} /L is in the range of the daily requirement of Cu(II) for a healthy adult, in an eventual dietary supplement formulation, requiring about 0.5 g of TPB with Cu (II) biosorbed [6,14].

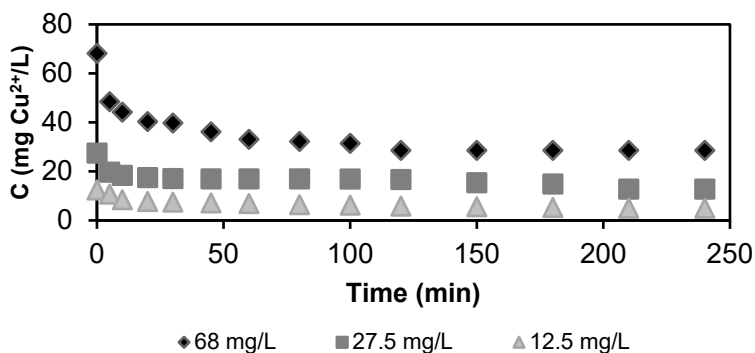


Figure 3. Cu(II) concentration time evolution for biosorption onto TPB; 1 g TPB, $C_i = 68$ mg Cu(II)/L, $d = 200\text{-}400$ μm , 296 K, pH = 5.41, 300 rpm.

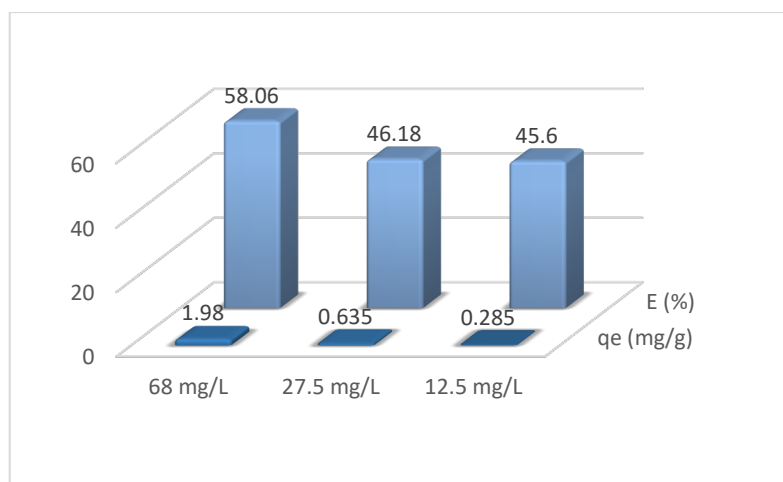


Figure 4. Initial concentration influence over equilibrium biosorption capacity (q_e) and biosorption efficiency (E,%) for Cu(II) biosorption on TPB; 1 g TPB/100 mL, $d = 200\text{-}400$ μm , 296 K, pH = 5.41, 300 rpm.

II.2. Effect of biomass quantity on the biosorption process

The effect of biomass quantity on Cu (II) biosorption was studied using different quantities of TPB powder, ranging from 1 to 3 g (Figure 5).

The increase in the biomass quantities, from 1 to 3 g, increases biosorption of Cu(II) ions onto TPB from 51.34% to 73.67%.

BIOSORPTION OF Cu (II) IONS USING RESIDUAL TOMATO POMACE BIOMASS.
A STUDY OF ISOTHERMS AND KINETICS

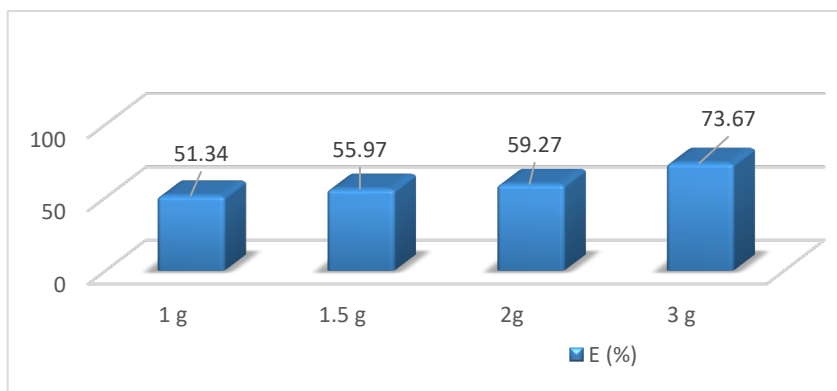


Figure 5. The effect of the TPB quantity on Cu (II) biosorption over the biosorption efficiency (E,%); ($C_i = 68 \text{ mg Cu(II)/L}$, $d = 200\text{-}400 \text{ }\mu\text{m}$, 296 K , $\text{pH} = 5.41$, 300 rpm).

More visible changes in the biosorption efficiency can be observed at quantities between 2 and 3 g. This effect could be explained by the availability of more adsorption sites on biosorbent surface and by increasing on total functional groups. Higher biomass quantities improve the biosorption efficiency, but not significantly, therefore the optimal amount of TPB for biosorption of Cu(II) was chosen to be 1 g TPB/100 mL Cu(II) solution for further experiments.

II.3. Effect of the stirring rate

Biosorption experiments were repeated with varying stirring speeds from 300 to 700 rpm (rotations per minute). As such, the curve for Cu (II) biosorption with respect to time, in terms of biosorption efficiencies, could be drawn for three different rotation speeds, 300, 500 and 700 rpm (Figure 6).

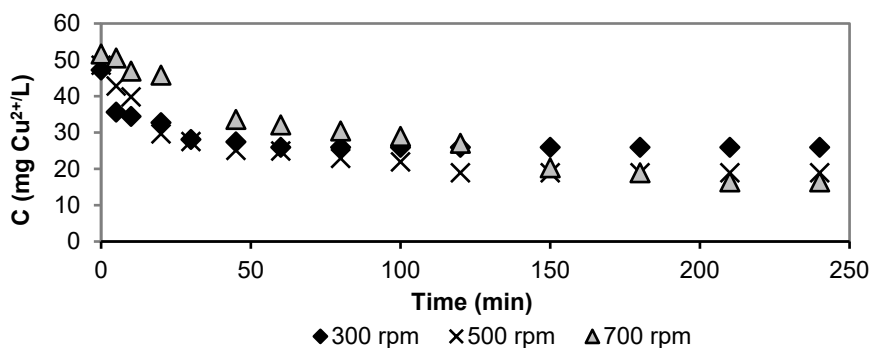


Figure 6. Influence of the stirring rate over time evolution of Cu (II) biosorption onto TPB ($C_i = 68 \text{ mg Cu (II) / L}$, 296 K , 1 g TPB , $d = 200\text{-}400 \text{ }\mu\text{m}$, $\text{pH} = 5.41$, 300 rpm)

The obtained curves showed that the biosorption process was intensified with stirring rate up to 500 rpm, but a further increase from 500 to 700 rpm will lead to a less increase, showing that after a certain stirring speed, the minimization of the thin film layer formed at the TPB surface will not lead to a further increase in the external diffusion rate.

As can be seen in Figure 7, even if the biosorption efficiency increases from 45.12 % to 65.21 %, by increasing the rotation speed from 300 rpm to 700 rpm, however, for energy saving reasons, for subsequent experiments the rotation speed of 300 rpm will be chosen.

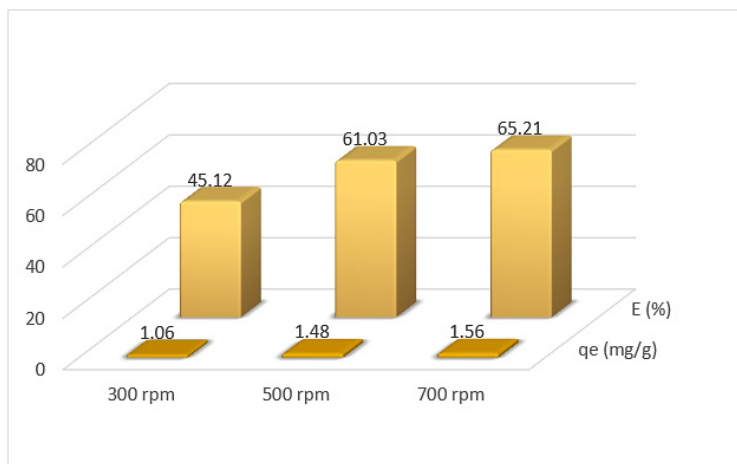


Figure 7. Influence of the stirring rate over the efficiency (E,%) and biosorption capacity at equilibrium (q_e , mg/g) of the Cu (II) retain onto TPB ($C_i = 68\text{mg/L}$, 296 K, $d = 200\text{-}400\ \mu\text{m}$, 1g TPB/100 mL, pH = 5.41, 150 min).

III. Adsorption isotherms

The adsorption isotherms describe the pathway of the interaction of a substrate from the bulk solution to the surface of adsorbate.

The equilibrium data were analysed using different isotherm models (Figures 8-11). In this article, four important isotherm models, namely Langmuir, Freundlich, Temkin and Dubinin–Radushkevich, were selected to fit the obtained experimental data. Each isotherm is characterized by definite constants whose values express the surface properties and affinity of the studied material.

There is a limitation of Langmuir equation because it assumes that adsorption is monolayer with no attraction between molecules on the surface of adsorbate.

BIOSORPTION OF Cu (II) IONS USING RESIDUAL TOMATO POMACE BIOMASS.
A STUDY OF ISOTHERMS AND KINETICS

Using Langmuir model, the maximum adsorption capacity (q_m) was found to be 2.959 mg g^{-1} (Table 1).

Temkin isotherm model takes into account the effects of indirect adsorbate/adsorbate interactions on the adsorption process; it is also assumed that the heat of adsorption (ΔH_{ads}) of all molecules in the layer decreases linearly as a result of increase surface coverage [15]. The Temkin isotherm equation has been applied to describe adsorption on heterogeneous surface.

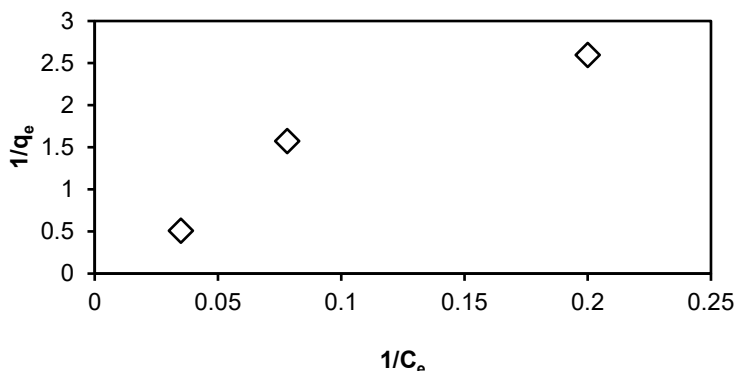


Figure 8. Langmuir plot for Cu^{2+} biosorption onto TPB ($C_i = 12.5\text{-}68 \text{ mg Cu}^{2+}/\text{L}$, 296 K , $\text{pH}=5.41$, 1 g TPB , $d = 200\text{-}400 \mu\text{m}$, 300 rpm).

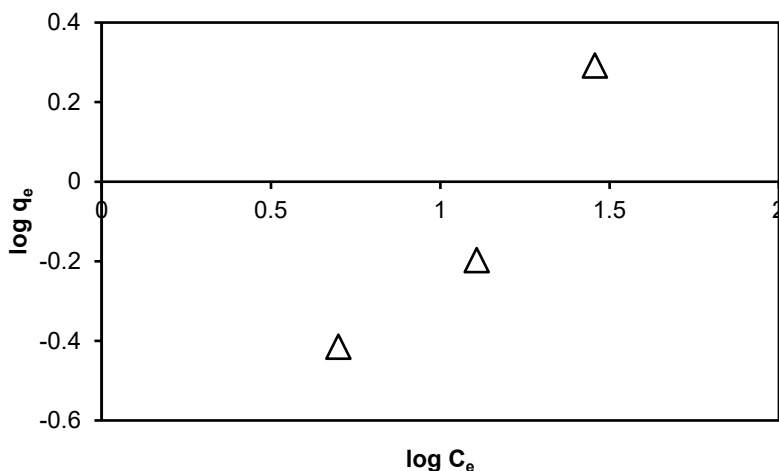


Figure 9. Freundlich plot for Cu^{2+} biosorption onto TPB ($C_i = 12.5\text{-}68 \text{ mg Cu}^{2+}/\text{L}$, 1 g TPB , $d = 200\text{-}400 \mu\text{m}$, 296 K , $\text{pH}=5.41$, 300 rpm).

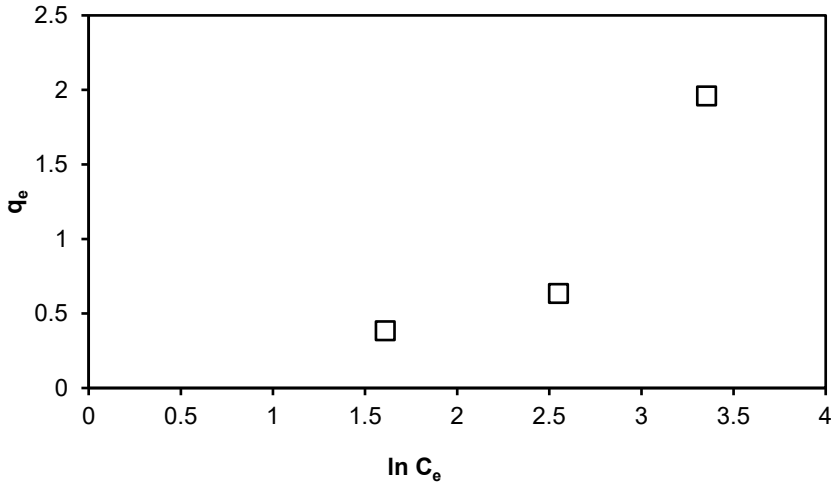


Figure 10. Temkin plot for Cu^{2+} biosorption onto TPB ($C_i = 12.5\text{-}68 \text{ mg Cu}^{2+}/\text{L}$, 296 K, $\text{pH}=5.41$, 1 g TPB, $d = 200\text{-}400 \mu\text{m}$, 300 rpm).

Therefore, by plotting q_e versus $\ln C_e$, enables the determination of the constants A_T and B . B is the Temkin constant related to heat of sorption (J/mol) and A_T is the Temkin isotherm constant (L/g) (Figure 10, Table 1).

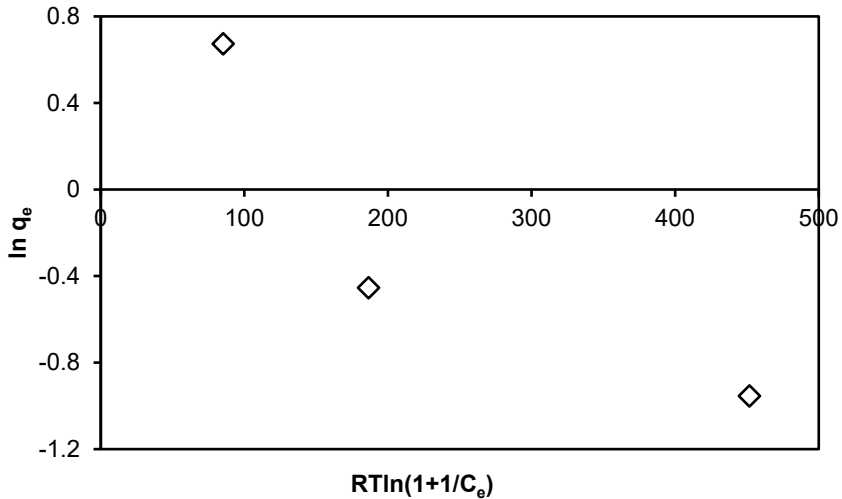


Figure 11. Dubinin–Radushkevich plot for Cu^{2+} biosorption onto TPB ($C_i = 12.5\text{-}68 \text{ mg Cu}^{2+}/\text{L}$, 296 K, $\text{pH}=5.41$, 1 g TPB/100 mL, $d = 200\text{-}400 \mu\text{m}$, 300 rpm).

Dubinin-Radushkevich isotherm model [16] is an empirical adsorption model that is generally applied to express adsorption mechanism with Gaussian energy distribution onto heterogeneous surfaces. This isotherm model was developed to account for the effect of the porous structure of the adsorbents. It was based on the adsorption potential theory and assumed that the adsorption process was related to micropore volume filling as opposed to layer-by-layer adsorption on pore walls.

Dubinin-Radushkevich isotherm model is superior to the Langmuir isotherm since it did not consider a homogeneous surface or constant adsorption potential [17]

It is usually applied to differentiate between physical and chemical adsorption of metal ions. A distinguishing feature of the Dubinin-Radushkevich isotherm is the fact that it is temperature dependent; hence when adsorption data at different temperatures are plotted as a function of logarithm of amount adsorbed versus the square of potential energy, all suitable data can be obtained [18].

From the linear plot of Dubinin-Radushkevich model, q_s was determined to 2.013 mg/g (Table 1). The mean free energy was calculated and has value $E = 16$ KJ/mol, that indicating a chemisorption process.

The coefficient of determination $R^2 = 0.89$ for Dubinin-Radushkevich model is higher than that of Tempkin model ($R^2 = 0.83$), so, the first is preferred.

From literature [19], is well-known that, if E value is between 8 and 16 kJ/mol, the adsorption follows an ion-exchange process (chemisorption), and if $E < 8$ kJ/mol, the adsorption process is physical.

Table 1. Langmuir, Freundlich, Temkin and Dubinin–Radushkevich coefficients calculated using linear regression analysis for Cu^{2+} adsorption on TPB; $C_i = 12.5$ -68 mg Cu^{2+}/L , 296 K, pH = 5.41, 1 g TPB/100 mL, $d = 200$ -400 μm , 300 rpm.

Langmuir			Freundlich			Temkin			Dubinin–Radushkevich		
b (L/mg)	q_m (mg/g)	R^2	n	K_f ($mg^{(1-1/n)}$ $L^{1/n}/g$)	R^2	B (J/mol)	A_T (L/g)	R^2	q_s (mg/g)	K_{ad} (mol^2/KJ^2)	R^2
0.028	2.959	0.92	1.084	0.077	0.93	0.885	0.999	0.83	2.013	0.002	0.89

IV. Kinetics models

The data obtained from adsorption kinetic experiments were simulated using five kinetic models, which are pseudo-first order, pseudo-second order reaction rate, Elovich, Weber-Morris intra-particle diffusion and Boyd external film diffusion models. Coefficient of correlation (R^2), which represent the percentage of variability in the dependent variable (the variance about the mean) is employed to analyse the fitting degree of isotherm and kinetic models with the experimental data [20] and as is well known, may vary from 0 to 1. The values of k_1 and q_e calculated from the slope and intercept obtained from the linear plot of $\ln(q_e - q_t)$ vs. t (Figure 12) and the R^2 values of fitting the first-order rate model at the three concentrations are presented in Table 2.

Linear plot of t/q_t vs. t (Figure 13) was used for calculating the q_e (cal) of pseudo-second order and k_2 , and these values are also shown also in Table 2.

IV.1. Pseudo-first-order kinetic model

This model – Lagergren [21] – describes the adsorption of one adsorbate molecule onto one active site of the biosorbent.

The constants K_1 and q_e were estimated from the slope and intercept by plotting $\ln(q_e - q_t)$ vs. time, respectively (see Figure 12 and Table 2). Calculated adsorption capacity values (q_e) of Cu (II) biosorption on TPB are much lower ($q_{\text{calc}} = 1.02$ mg/g, Table 2) in comparison to experimental ones ($q_e = 1.98$ mg/g, Figure 4) and R^2 (regression coefficient) values are small (no. 0.74, Table 2), suggesting that the pseudo-first-order model cannot describes the studied system.

IV.2. Pseudo-second-order kinetic model

Experimental data were also tested using the Ho and McKay [22] pseudo-second-order equations. The rate constants (k_2), R^2 and q_e values are given in Table 2, Figure 13.

As the table shows, the linearized pseudo second-order kinetics model provides much better R^2 values (0.999 for all tree concentrations) than those for the pseudo-first-order model.

The good agreement between the experimental data and the pseudo-second order kinetic model (Figure 13, Table 2) show that in the studied biosorption process, the rate-limiting step is the chemical interaction between the Cu(II) ions and the functional groups on the TPB biosorbent surface. Moreover, for retention on the biosorbents surface, Cu(II) ions need two functional groups, which must be geometrically favorable.

BIOSORPTION OF Cu (II) IONS USING RESIDUAL TOMATO POMACE BIOMASS.
A STUDY OF ISOTHERMS AND KINETICS

Since studied TPB biosorbent has a large number of functional groups on their surface (FTIR analysis, Figure 1), it can be assumed that there is no reason why biosorption should not takes place according to the pseudo-second-order kinetics.

The theoretical q_e (cal) = 2.05 mg/g for C_i = 68 mg Cu (II)/L (Table 2) value were also found in concordance with the experimental value q_e (exp) = 1.94 mg/g for the C_i = 68 mg Cu (II)/L (Figure 4).

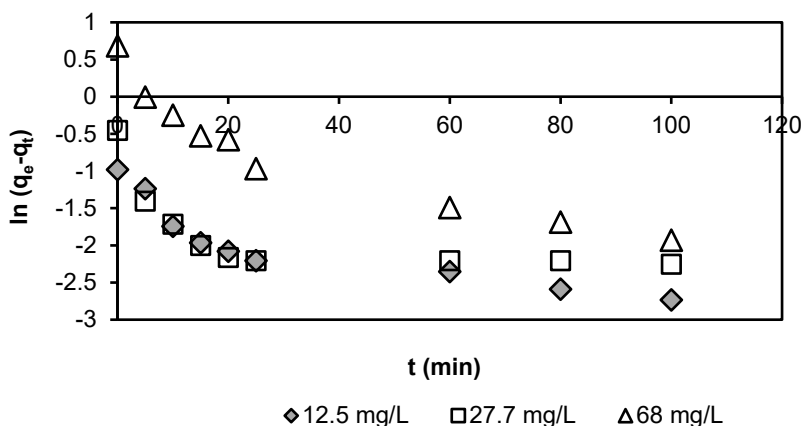


Figure 12. Plots of the pseudo-first-order kinetic models for Cu (II) biosorption using TPB; C_i = 12.5-68 mg Cu^{2+} / L, 1g TPB/100 mL, d = 200-400 μm , 296 K, pH = 5.41, 300rpm.

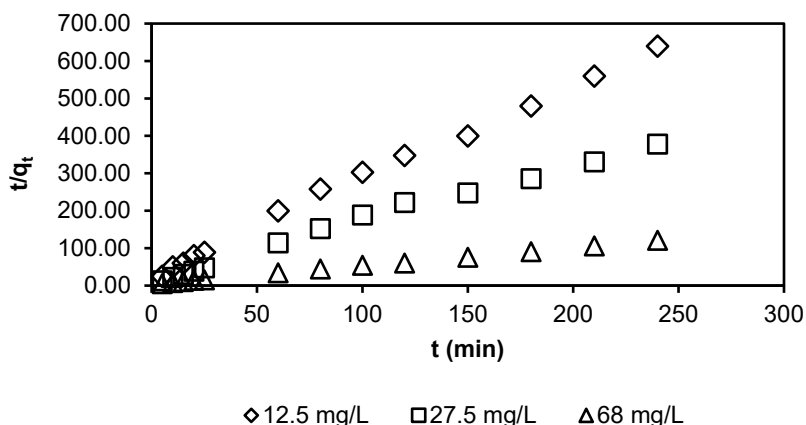


Figure 13. Plots of the pseudo-second-order kinetic models for Cu (II) biosorption using TPB; C_i = 12.5-68 mg Cu^{2+} / L, 1g TPB, d = 200-400 μm , 296 K, pH = 5.41, 300rpm.

IV.3. Elovich equation

The Elovich equation has been widely used in adsorption kinetics, which describes chemical adsorption (chemical reaction) mechanism in nature. The model of Elovich and Larinov [23] is based on a kinetic principle assuming that the adsorption sites increase exponentially with adsorption, which implies a multilayer adsorption.

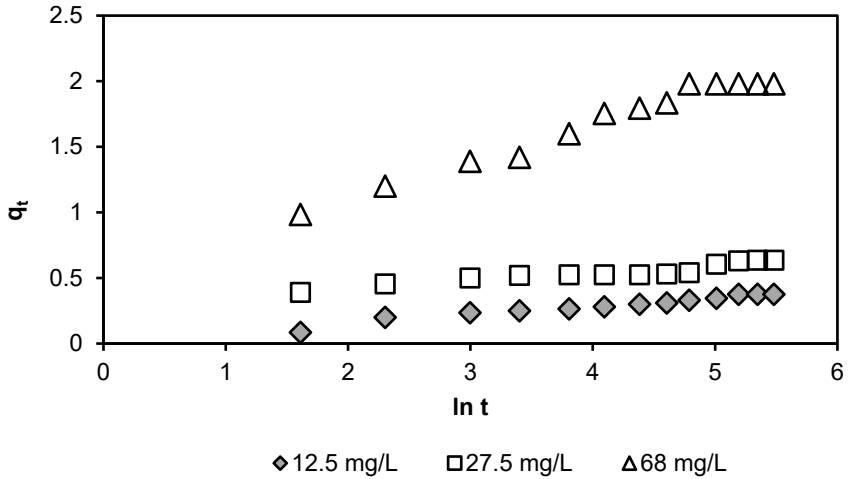


Figure 14. Elovich plots for Cu^{2+} biosorption onto TPB ($C_i = 12.5\text{--}68 \text{ mg Cu}^{2+}/\text{L}$, $1 \text{ g TPB}/100\text{mL}$, $d = 200\text{--}400 \mu\text{m}$, 296 K , $\text{pH}=5.41$, 300 rpm).

Table 2. Pseudo-first-order, pseudo-second-order rate constants and Elovich kinetic models calculated and experimental q_e values for Cu (II) biosorption onto TPB using different initial concentrations; $C_i=12.5\text{--}68\text{mg Cu}^{2+}/\text{L}$, $1\text{g TPB}/100 \text{ mL}$, $d=200\text{--}400 \mu\text{m}$, 296K , $\text{pH} = 5.41, 300 \text{ rpm}$.

Concentration (mg Cu^{2+}/L)	Pseudo-first order			Pseudo-second order			Elovich		
	q_m (mg/g)	K_{ad} (min^{-1})	R^2	q_m (mg/g)	K_2 (g/mg·min)	R^2	α (mg/g·min)	β (g/mg)	R^2
12.5	0.224	0.014	0.74	0.391	0.215	0.99	0.081	14.025	0.95
27.5	0.225	0.010	0.37	0.643	0.172	0.99	1.394	7.85	0.90
68	1.018	0.022	0.85	2.052	0.061	0.99	2.093	3.63	0.97

In the case of Elovich kinetic model, the low values of the correlation coefficients, between 0.90 and 0.97 (see Figure 14, Table 2), suggest that this model is not suitable to describe the Cu(II) on TPB biosorption process.

IV.4. Intra-particle diffusion kinetic model

This model was developed by Weber and Moris, in 1962 [24]. According this model, adsorption is a mass transport process that can be viewed as a diffusion. The adsorption mechanism is through three steps, i.e., the external mass transfer, the intraparticle diffusion, and the final equilibrium step [25, 26].

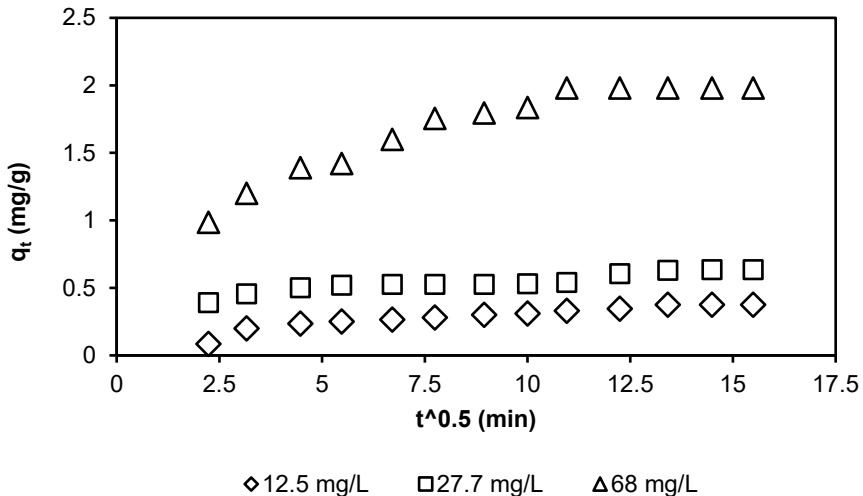


Figure 15. Intraparticle diffusion kinetics for biosorption of Cu(II) onto TPB at 296K.

The intra particle diffusion Weber and Morris [24] was considered in order to establish how mass transfer through the biomass pores influences the biosorption process.

Plots of q_t against $t^{1/2}$ are linear, but with intercepts +0.13, +0.90 and +1.94 (Table 3), suggesting that early stages of the diffusion process could be rate-limitative at small concentrations ($C_i = 12.5$ mg Cu (II)/L).

IV.5. External diffusion kinetics model.

The external diffusion models assume that the diffusion of adsorbate in a bounding liquid film around the adsorbent is the slowest step.

Several equations have been developed to model the external mass transfer process.

Boyd's external diffusion model [27] simulates the external diffusion of adsorbate in a liquid film.

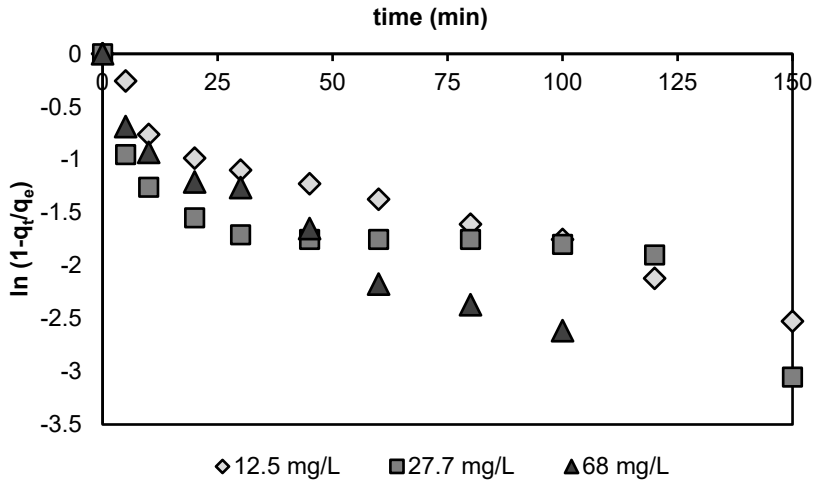


Figure 16. Boyd's external diffusion kinetics model for biosorption of Cu(II) onto TPB at 296K.

The liquid film model [27] plots $(-\ln(1 - q_t/q_e))$ against t do not exhibit zero intercepts (Table 3, +0.44, +0.61 and +0.53), suggesting that the process is not controlled by diffusion through the liquid film surrounding the TPB biosorbent particles.

Table 3. Intra-particle and external (film) diffusion rate coefficients for Cu^{2+} biosorption on TPB; 12.5 - 68 mg Cu^{2+}/L , 300 rpm, 296 K. pH = 5.41.

Concentration (mg Cu^{2+}/L)	Intra-particle diffusion			External (Film) Diffusion		
	K_p (min^{-1})	Intercept	R^2	K_{fd} (min^{-1})	Intercept	R^2
12.5	0.178	0.128	0.87	0.014	0.439	0.91
27.5	0.015	0.900	0.88	0.012	0.613	0.97
68	0.072	1.038	0.87	0.023	0.529	0.91

CONCLUSION

In the present work, a modified biomass (TPB) for biosorption of Cu(II) ions from aqueous solution, in a batch adsorption study was investigated, in order to obtain a biomaterial that could be used as a base for a dietary supplement with Cu(II) and significant amounts of lycopene from TPB.

The surface modifications after Cu(II) biosorption on TPB were analysed by the FTIR and SEM analyses.

The biosorption Cu(II) ions on TPB depends on the initial Cu(II) ions concentration, contact time and stirring rate. 68 mg/L of biosorbent dose, 150 min of contact time and 300 rpm, at room temperature for Cu(II)/TPB system was used. The adsorption of Cu(II) ion from aqueous solution increased with increase in the contact time. The biosorption percentage of Cu(II) ions increased with increase with the biosorbent quantity and stirring rate. However, for energy saving reasons, the rotation speed of 300 rpm will be chosen.

The adsorption kinetics and mechanism were analysed by using kinetic models such as pseudo-first-order, pseudo-second-order, Elovich, intraparticle diffusion and external diffusion film model.

The pseudo-second-order was fitted very well compared to all other kinetic models.

Freundlich model was fitted well with the maximum R^2 value (0.93) compare to Langmuir, Temkin and Dubinin-Radushkevich models for TPB.

Taking into consideration that pore diffusion coefficients have higher values than the rate-determining range, that none of the plots of the liquid film model exhibit a zero intercept, and that the biosorption fits the pseudo-second-order kinetics, the considered process that takes place is chemisorption.

Finally, we concluded that TPB biosorbent is an effective material to adsorb the Cu(II) ions from aqueous solution.

Taking into consideration the values obtained for the adsorption capacity and knowing the WHO suggested intake of copper for males and females, 0.5 g of TPB, in powder form containing Cu(II), could be used as a dietary supplement in order to supply the daily copper demand of the organism.

EXPERIMENTAL SECTION

Materials

The stock solution, 1 g/L of Cu (II), was prepared by dissolving $\text{CuSO}_4 \cdot 5\text{H}_2\text{O}$ in distilled water. Analytical grade, without further purification, from E. Merck Ltd., Germany was used. The required concentrations were obtained by diluting the stock solution to the desired concentrations, in 12.5–68 mg Cu^{2+} /L range.

The tomato waste material (peel, seeds and pulp), TPB, required as starting material for this work was collected locally, after tomato juice extraction. Initially, for the preparation of biosorbent, the biomass was crushed, washed several times with distilled water, and dried in the oven at 70 °C, for 48 h until the biosorbent constant weight is obtained. The dried TPB samples were ground to fine powder and the this was sieved through different sizes and 200–400 μm fractions was used. This was stored in a desiccator and used in further experiments.

Biosorption experiments.

Biosorption process took place under established conditions in a beaker (thermostated batch conditions, 296K ±2K) containing 100 mL of Cu (II) solution of different concentrations (12.5–68 mg/L) and different quantities (1–3 g) of TPB. The different solutions were placed on a magnetic stirrer and stirred at a different speed (300-700 rpm) in a continuous manner. In order to determine the exact concentration of copper and to establish the evolution of the biosorption process, water samples from the supernatant, diluted as required, were collected at different time intervals, until equilibrium was reached. The maximum contact time used was 240 min to ensure that biosorption equilibrium was reached.

The concentration of copper ions in the solution was determined using a flame atomic absorption spectrophotometer (Sens AA Dual GBS Scientific Equipment, Australia).

Biosorption efficiency, expressed as percentage, was calculated with equation (1):

$$E = \frac{C_0 - C_e}{C_0} \times 100 \quad (1)$$

where C_0 and C_e are the initial and equilibrium concentrations of Cu (II), respectively (mg/L).

The amount of Cu(II) biosorbed per gram of TPB (mg/g) was calculated using equation (2):

$$q_e = \frac{(C_0 - C_e) \cdot V}{m} \quad (2)$$

where V is solution volume (L) and m is TPB quantity (g).

All parametrical values presented are the averaged mean of three series of data recorded from repetitions of the same experiment.

REFERENCES

1. G. Giovanelli and A. Paradiso, *J. Agric. Food Chem.*, **2002**, *50*, 7277–7281; doi.org/10.1021/jf02559r.
2. Z. Lu, J. Wang, R. Gao, F. Ye, G. Zhao, *Trends Food Sci. Technol.*, **2019**, *86*, 172-187.
3. G.S. Dhillon, S. Kaur, H.S. Oberoi, M.R. Spier, S.K. Brar, Chapter 2 -Agricultural-Based Protein By-Products: Characterization and Applications; in Protein byproducts, Academic Press, **2016**, p21-p36; doi.org/10.1016/B978-0-12-802391-4.00002-1.
4. F. Jiang, Y.-L. Hsieh, *Carbohydrate polymers*, **2015**, *122*, 60-68.
5. G. Toscano, A. Pizzi, E. Foppa Pedretti, G. Rossini, G. Ciceri, G. Martignon, D. Duca, *Fuel*, **2015**, *143*, 89-97.
6. <https://www.healthline.com/nutrition/food-high-in-copper>
7. Wiecek, S., Paprocka, J., *Metabolites*, **2024**, *14*, 38-51.
8. S. Azabou, I. Louati, F. Ben Taheur, M. Nasri, T. Mechichi, *Environ. Sci. Pollut. Res.*, **2020**, *27*, 39402–39412.
9. A.Ş. Yargıç, R.Z. Yarbay Şahin, N. Özbay, E. Önal, *J. Clean. Prod.*, **2015**, *88*, 152-159.
10. M. Changmai, P. Banerjee, K. Nahar, M. K. Purkait, *J. Environ. Chem. Eng.*, **2018**, *6*, 246-257.
11. H. Saygılı, F. Güzel, Y. Onal, *J. Clean. Prod.*, **2015**, *93*, 84–93.
12. H. Saygılı, F. Güzel, *J. Clean. Prod.*, **2016**, *113*, 995–1004 K. Y.
13. Pandya, R. V. Patel, R. T. Jasrai, N. Brahmhatt, *Int. J. Eng. Res. Gen. Sci.*, **2017**, *5(4)*, 137-148.
14. N. Ayawei, A. N. Ebelegi, D. Wankasi, *J. Chem.*, **2017**, *7*, 1-11.
15. C. Indolean, A. Măicăneanu, M. Cristea, *The Canadian Journal of Chemical Engineering*, **2017**, *95*, 615-622.
16. N. Ayawei, A. Newton Ebelegi, D. Wankasi, *J. Chem.*, **2017**, *50*, 1-11.
17. Qi. Hu, Z. Zhang, *J. Mol. Liq.*, **2019**, *277*, 646-648.
18. A. G`unay, E. Arslankaya, I. Tosun, *J. Hazard. Mat.*, **2007**, *146(1-2)*, 362–371M. A Al-Ghouti, D. A. Da'ana, *J. Hazard. Mat.*, **2020**, *393*, 122383-122392.
19. A. Sari, M. Tuzen, *J. Hazard. Mater.*, **2008**, *152*, 302 308.
20. N. Bar, T. Mitra, S. K. Das, *J. Environ. Eng. Land. Manag.*, **2021**, *29 (4)*, 441–448.
21. Lagergren, S., *Royal Swed. Acad. Sci.* **1898**, *24*, 1–39.
22. Ho, Y.S.; McKay, G., *Process Biochem.* **1999**, *34*, 451–65.
23. S.Y. Elovich, O.G. Larinov, *Izv. Akad. Nauk. SSSR, Otd. Khim. Nauk*, **1962**, *2*, 209–216.
24. W.J. Weber, C.J. Morris, *Proceed. Intern. Conf. Water Poll. Symp.* Oxford: Pergamon Press, **1962**, *2*, 231-266.
25. Y. Qu, C. Zhang, F. Li, X. Bo, G. Liu, Q. Zhou, *J. Hazard. Mat.*, **2009**, *169(1–3)*, 146–152.
26. R. Ratnawati, A. Prasetyaningrum, H. Hargono, M. F. Zakaria, *Period. Politech. Chem. Eng.*, **2023**, *10*, 1-14.
27. G.E. Boyd, A.W. Adamson, L.S. Jr. Myers, *J. Am. Chem. Soc.*, **1947**, *69*, 2836–2842.